On the Potential of Wireless Sensor Networks for the In-Field Assessment of Bio-Physical Crop Parameters

Jan Bauer•, Bastian Siegmann°, Thomas Jarmer°, and Nils Aschenbruck•

•University of Osnabrück
Institute of Computer Science
Albrechtstr. 28, 49076 Osnabrück, Germany
{aschenbruck, bauer}@uos.de

°University of Osnabrück
Institute for Geoinformatics and Remote Sensing
Barbarastr. 22b, 49076 Osnabrück, Germany
{tjarmer, bsiegmann}@igf.uos.de

***Abstract*—The exploration of bio-physical crop parameters is fundamental for the efficiency of smart agriculture. The leaf area index (LAI) is one of the most important crop parameters and serves as a valuable indicator for yield-limiting processes. It contributes to situational awareness ranging from agricultural optimization to global economy. In this paper, we investigate the potential of Wireless Sensor Networks (WSNs) for the in-field assessment of bio-physical crop parameters. Our experiences using commercial off-the-shelf (COTS) sensor nodes for the indirect and nondestructive LAI estimation are described. Furthermore, we present the design of our measurement architecture and results of various in-field measurements. By directly comparing the results achieved by WSN technology with those of a conventional approach, represented by a widely used standard instrument, we analyze whether bio-physical crop characteristics can be derived from WSN data with a desired accuracy. Moreover, we propose a simple approach to significantly enhance the accuracy of COTS sensor nodes for LAI estimation while, at the same time, reveal open challenges.**

I. Introduction

Agriculture is facing crucial challenges due to climate change. Adapted crop types may have to be selected and fertilization as well as irrigation has to be modified because of less precipitation and higher temperatures. In general, an earlier situational awareness will have a positive impact such as: (1) Optimization of fertilizer and irrigation applications, (2) Optimization of harvester operational modes. Moreover, in extreme situations, low yield rates would be known earlier and allow to secure the supply on the world market. To realize situational awareness, there is a demand for advanced sensor technology to explore the bio-physical and bio-chemical characteristics of crop in the field.

The estimation of crop characteristics such as fractional cover, biomass, leaf area index (LAI), and fraction of absorbed photosynthetically active radiation (fPAR) can be derived with physical models, which use the principles of how irradiance is absorbed by plants. In this context, the LAI is one of the most important bio-physical plant parameters and a key variable for models in climatology, meteorology, ecology and agronomy [1]. It is defined as the ratio of foliage area to the ground area (m^2 foliage / m^2 ground) and is an indicator for the photosynthetic performance of plants [5], [7], [12]. Thus, the LAI is used as an integrative measure of the influence of biotic and abiotic conditions in agronomical modeling. This measure provides important information for yield models, since it serves as an indicator for yield-limiting and -reducing processes caused by plant diseases and mismanagement [2], [4], [6], [22].

Various methods have been developed for determining the LAI in recent years. These methods differ in the type of measurement methodology and in the requirements of the technical equipment. Although, destructive assessment of the LAI usually provides more precise results, this direct data acquisition is time-consuming, expensive, and, therefore, limited to small areas [3], [12]. Alternatively, the LAI is often measured nondestructively in-field with specific instruments (e.g., LAI-2000/2200 (LI-COR Inc., USA), SunScan device (Delta-T Devices Ltd., USA)) [7], [8], [21] or derived from remote sensing images (satellite or airborne) [2], [11]. In both ways, the temporal as well as spatial resolution is quite low. Furthermore, the costs for the acquisition of satellite or airborne images are rather high and limit the temporal resolution as well.

Wireless Sensor Networks (WSNs) consists of low cost and low-power computing devices equipped with sensors that form a self-organizing network to collect data. These networks are designed for long-term and large-scale deployments. Hence, they are highly suitable for in-situ monitoring of crop parameters and smart agriculture as a whole. This has been realized by research since almost one decade, cf. [14], and a promising progress has already been made in the context of in-field assessment of crop characteristics [20], [23].

The individual sensor device is rather inexpensive and measures simple physical parameters (e.g., ambient light, temperature, or humidity) with limited accuracy. This lack of accuracy is compensated by the plurality of collaborating devices. Within a WSN, the sensor information of all devices is gathered, fused, and forwarded to a central instance possibly connected to the Internet. Thus, WSNs can continuously deliver sensor data at high temporal as well as spatial resolution. Eventually, they have the potential to reduce the time and labor costs for conventional in-field data acquisition.

 DOI: 10.1109/LCNW.2014.6927698

In this paper, we describe our experiences of indirect LAI assessment based on solar transmittance of plant canopy by using commercial off-the-shelf (COTS) sensor nodes. We introduce results of various in-field measurements including an analysis whether bio-physical crop characteristics can be calculated from WSN data with the desired accuracy. For that purpose, we directly compare the results achieved by sensor nodes with those of a widely used standard instrument. At the same time, we reveal open challenges for accuracy and identify a first approach for accuracy improvements.

The rest of this paper is organized as follows: Section II surveys related agriculture WSN deployments and the work which has been done in the context of in-field LAI monitoring. The basic model of indirect LAI estimation is introduced in Section III. In Section IV, we describe our measurement architecture including hardware and implementation details. Then, we present the results of field trials in Section V. In Section VI, we introduce and validate our approach to enhance the potential of LAI estimation using WSNs. Finally, Section VII concludes the paper and provides our plans for future work.

II. Related Work

In [14], Langendoen et al. share preliminary experiences with deploying a WSN for precision agriculture. The paper reveals many engineering difficulties and emphasizes demands of research in fundamental functionalities of large-scale and long-term WSN deployments. But in contrast to our intention, the authors study temperature and humidity within a crop canopy to prevent potatoes from fungal disease.

Another early WSN application for environmental monitoring, GreenOrbs, is introduced in [16]. The authors address the task of canopy closure estimation in forests using optical sensors to discriminate the states between light and shade. Moreover, a technique for sensor calibration is proposed. Besides, the authors investigate the environmental impact on link quality and network topology, respectively, and provide an estimation of power consumption of their prototype.

In [23], pioneering research of indirect LAI measurement using sensor node technology is presented allowing low-cost WSN crop monitoring. The authors focus on an iterative scheme to deploy sensor nodes into farmland. They show promising results in simulations and field tests. However, the obtained LAI is not compared to conventional standard instruments.

A continuous LAI monitoring system based on WSNs is proposed in [21]. It is shown that a proper measurement timing is necessary for an accurate LAI determination in order to avoid direct sunlight when using a nondestructive method. Therefore, a practical timing approach is presented and demonstrated in a tomato greenhouse.

Recently published, Qu et al. present an agriculture WSN for LAI monitoring [20]. Based on preliminary work [19], a custom sensor node platform has been designed which subsequently was deployed in an experimental maize field. The authors also introduce an algorithm for LAI retrieval using sensor nodes. The values obtained during one month of observation are compared with selective conventional estimates and satellite observation data, confirming the potential of indirect LAI estimation by WSNs for validating remote sensing data.

Similar to [21], our goal is to use a COTS sensor platform and to validate the results for different kind of crop with standard instrumentation as in [20].

III. Theoretical Background

We focus on an indirect methodology for LAI determination by gap fraction analysis, i.e., by measuring the solar transmittance of plant canopy which is also investigated in [19], [21], [23]. Spectral reflectance and transmittance of plants in the visible region of the electromagnetic spectrum is primarily affected by pigments (e.g. chlorophyll and carotinoids). Green vegetation has a very low level of reflectance and transmittance in the range of blue (400–490 nm) and red light (680–770 nm) because plants strongly absorb the energy of this part of radiation to carry out photosynthesis. In the range of green light (490–580 nm), reflectance and transmittance are higher as less radiation is absorbed by the pigments.

This typical behavior of light transmittance of plants in the visible spectrum is leveraged by the indirect LAI determination. The *Beer-Lambert law* establishes the theoretical basis to derive LAI from the quantitative interaction between the solar radiation and the plant canopy, cf. [12]. According to that law, there is a logarithmic dependency between the LAI (L) and the solar radiance partially absorbed by the canopy which can be described by the following equation:

$$B = Ae^{-CL}. \tag{1}$$

Here, A is the light intensity observed above-canopy and B the corresponding sensor reading below-canopy. Furthermore, the constant term C is the light *extinction coefficient* which is given by the quantity of the specific light absorption property of plant's leaves. In addition, the leaf orientation angle and the solar altitude have an significant impact on this coefficient. Thus, it is both cultivar- and site-specific [12], [19].

By exponential transformation of Equation 1, the *Monsi-Saeki model* [17] which is also used in [23] and [19] applies the Beer-Lambert law for LAI estimation. This results in

$$L = -\frac{1}{C} log\left(\frac{B}{A}\right), \tag{2}$$

where $\frac{B}{A}$ is the *transmittance* which is used by the indirect methodology and gathered by standard optical instruments, e.g., LAI-2200, or digital hemisphere photography devices. Since these devices often do not take the scattered radiation from leaf surfaces into account, it is recommended to measure the light intensity under fully diffused sky conditions [13]. A method for properly determine the measurement timing in order to achieve these conditions is presented in [21]. However, there exist more sophisticated approaches to remove the scattered radiation effect in LAI measurements, e.g., [13].

An inherent weakness of the LAI estimation approach based on gap fraction analysis is that it does not distinguish

photosynthetically active leaves from other plant elements such as branches and stems [12]. Therefore, occasionally, the term *effective LAI* [5] is used to describe the LAI derived from the gap fraction method.

IV. Measurement Architecture

A. Wireless Sensor Nodes

We performed several tests with three different IEEE 802.15.4 compliant COTS sensor nodes: (1) TelosB [18], (2) MicaZ (Memsic, USA), and (3) G-Node (SowNet, NL). We compared the results of their sensor readings with regard to the LAI estimation. Whereas the TelosB features some onboard sensors, both MicaZ and G-Node require appropriate sensor boards, e.g., MTS310 or MTS400. Comparing these sensor boards with the onboard sensors of TelosB (Hamamatsu S1087 photodiode [10] and Sensirion SHT11 digital humidity and temperature sensor), we came to the conclusion that the TelosB photodiode (also used in [16], [21]) is more applicable for an in-field light intensity measurement required by the LAI estimation according to Equation 2, in particular under natural light conditions. This photosynthetically active radiation (PAR) sensor has a spectral response rage from 320 to 730 nm with a peak sensitivity wavelength at 560 nm [10]. Thus, it covers the visible range required for LAI estimation, cf. Section III.

B. Standard Instrumentation

In order to validate the LAI results gathered by the WSN, we use the LAI-2200 [15]. This instrument is one of the standard measuring devices for the nondestructive assessment of LAI and other canopy parameters in agricultural research. The instrument consists of a measurement wand which is attached to a control unit. At the end of the measurement wand, there is a fish-eye optical sensor. The sensor's field of view is divided into five rings with different center angles: 7 °, 23 °, 38 °, 53 °, and 68 ° visualized in Figure 1. Note that each ring has a range of roughly 12 ° resulting in an overall field of view of 148 ° [15].

A usual measurement of the LAI-2200 consists of a number (N_{obs}) of above canopy readings (A_{ij}) to measure the total incoming light and the corresponding number of below canopy readings to capture the rest of the incoming light (B_{ij}) which was not reflected or absorbed by the canopy. From the above and below measurement pairs the transmittance ($\overline{P(\theta_i)}$) for each ring i is calculated by:

$$\overline{P(\theta_i)} = \frac{1}{N_{obs}} \sum_{j=1}^{N_{obs}} \frac{B_{ij}}{A_{ij}} \,. \tag{3}$$

Subsequently, the LAI (L) can be determined with

$$L = 2 \int_0^{\pi/2} -\frac{\overline{lnP(\theta)}}{S(\theta)} sin\theta d\theta = 2 \sum_{i=1}^{5} \overline{K_i} W_i \,, \tag{4}$$

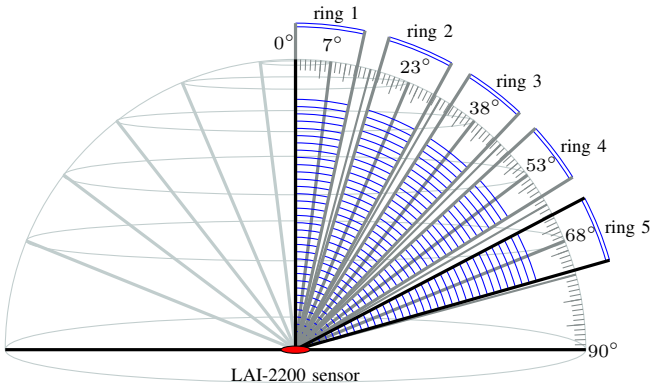

Fig. 1. The field of view of the LAI-2200 divided in five rings with different center angles, cf. [15].

where

$$\overline{K_i} = \frac{1}{N_{obs}} \sum_{j=1}^{N_{obs}} \frac{-ln\left(\frac{B_{ij}}{A_{ij}}\right)}{S_i} \text{ and } W_i = sin\theta_i d\theta_i \,. \tag{5}$$

$\overline{K_i}$ represents the mean contact frequency of the i-th ring. The factors S_i and W_i are specific weightings for the individual rings, both increasing from the first (7 ° center angle) to last ring (68 ° center angle). See [15] for more details.

To ensure accurate LAI measurements four major assumptions must be met, see [8], [15]:

1) The foliage is black (black body assumption). An optical filter rejects any radiation > 490 nm. In this range of the electromagnetic spectrum, reflectance and transmittance of foliage is very low.
2) The foliage is randomly distributed within certain foliage-containing envelopes.
3) Compared to the area of view of each ring the foliage elements are small.
4) The foliage has a random azimuthally orientation.

C. Measurement Setup

The practical meaning of Equation 2 in Section III is that a pair of optical sensors (one placed above and the other one below the canopy) allow LAI estimation as done by the LAI-2200. Hence, at the beginning of our measurement campaign in the spring of 2013, we deployed two TelosB sensor nodes in a wheat field using the setup depicted in Figure 2(a). The sensor node on a tripod samples its optical sensor regularly. At the same time it acts as a data sink for a second sensor which is placed under the canopy on top of a 20 cm brace. The sensor data received is forwarded to a gateway node attached to a laptop for further processing.

Note that sensor readings are inherently error-prone due to various instrumental issues. Nevertheless, Mo et al. [16] show that errors from individual sensors are consistent over time and, thus, linearly correlated and calibratable. Hence, sensor

(a) Pair setting with one TelosB on a tripod above and a second one below the canopy (red ellipse) deployed in a wheat field.

(b) Setting for the direct comparison of WSN versus conventional hardware using a TelosB mounted on the LAI-2200 wand.

Fig. 2. Measurement setups used for indirect LAI estimation.

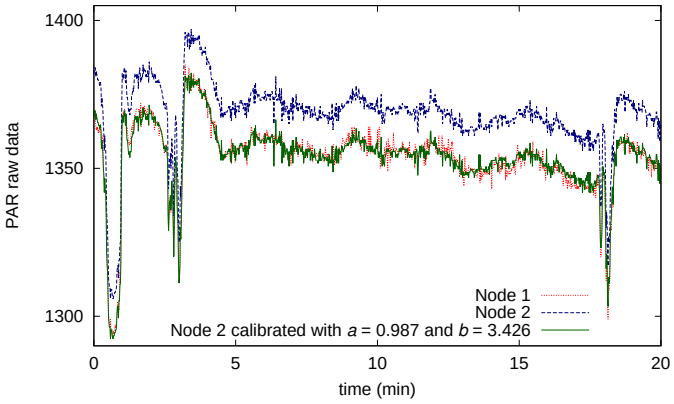

Fig. 3. Calibration of two TelosB optical PAR sensors under the same illuminance using the Pearson product-moment correlation according to [16].

calibration is very important to prevent incorrect measurements and should be conducted in regular intervals. In our deployment, we used the Pearson product-moment correlation method (similar to [16]) to calibrate both sensors. Figure 3 depicts the results of the calibration process. The readings of Node 2 are calibrated using the correlation coefficients a (gain) and b (offset) and Node 1 as a reference node.

We used this setup for measurements in the wheat field. Unfortunately, we were not able to reproduce the linear relation between the LAI measured by these WSN nodes and the LAI-2200, observed by [20]. Therefore, we decided to conduct further measurements estimating the LAI in maize fields (similar to [20]) and to modify our setup. In order to exclude potential error sources and inaccuraciesy by deploying two sensor nodes, we limited the new setup to a single node directly mounted on the measurement wand of the LAI-2200 (Fig. 2(b)), i.e., we use the same sensor for above and below data acquisition, simultaneously to the corresponding acquisition of the LAI-2200 instrument. By doing so, we try to achieve a higher accuracy and to clarify the relation between both devices.

D. Sensor Node Application

We implemented the sensor nodes' data acquisition application on the TelosB platform using *TinyOS* 2.1.2, a widely used open source operating system designed for low-power wireless devices, such as those used in WSNs. Although the temperature and the humidity is not directly required for the LAI estimation, we decided to already include these factors in our application since both enable an inference about climatological and agricultural conditions and could be used in the future.

Within the application, each sensor is sampled as often as possible in round-robin fashion. First, the photosynthetically active radiation (PAR) sensor is requested which takes 17.7±0.3 ms. Then, readings from the temperature and the humidity sensor are gathered inducing a latency of 242.1±0.4 ms and 78.0±0.1 ms, respectively. Hence, we obtain a sampling rate of roughly 3 Hz which is sufficient for our purpose. The LAI computation is done by a fully-equipped device (e.g., a generic laptop or smartphone) as central instance since the data has to be fused, in particular in case of distributed sensors (setup depicted in Figure 2(a)). Thus, the readings of individual sensors are transmitted to that data sink. For distributed sensors, the transmission costs energy as well as processing time. A sample-wise transmission is not reasonable. We therefore choose the maximum packet size and combine (temporarily buffered) readings in a batch of 17 samples of each sensor type per packet. This data packet is then broadcasted every 5.798±0.003 s to the corresponding sink. To achieve a more effective utilization of the communication channel, we plan to implement sophisticated data aggregation in the future.

Overall, the application consumes roughly a third of ROM available on TelosB (16.932 kB) and less than 8 % of RAM (780 byte) leaving enough memory for data aggregation, time synchronization, and routing protocol extensions which are intended to integrate for a long-term deployment.

E. Data Sink Application

The central data sink is realized by a sensor node which is connected with a fully-equipped device via USB and acts as a WSN gateway (using the TinyOS *BaseStation* application). On the fully-equipped device, the readings of individual PAR sensors are averaged (mean). In our measurement, we form the average of three consecutive data packets, each with 17 readings. Using the means, the transmittance (ratio of below and above canopy sensor readings) is determined and finally, the LAI of individual pairs of sensors is computed according to Equation 2.

In order to facilitate a more convenient deployment of sensor nodes and to enable in-situ error diagnostics, we developed an *Android* application for smartphones and tablets, respectively. This application records the sensor data packets

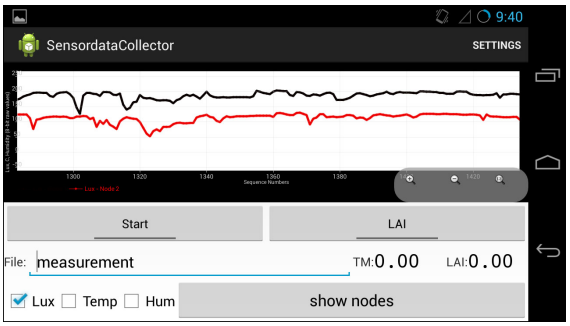

Fig. 4. Screenshot of the data-sink Android application visualizing two sensor data streams.

gathered by a sink sensor node attached via USB to the Android device. As we use the USB port, the device needs to support the USB host mode. Furthermore, the required FTDI drivers have to be included in the kernel. Using *AChartEngine*, the individual sensor readings are visualized in the GUI as shown in Figure 4.

Currently, the application is tailored to the TelosB platform and the packet format used in our deployment. Thus, light, temperature, and humidity raw values are assumed and can independently visualized in the graph using the corresponding buttons. Besides the visualization, the application can log the sensor data on the device or directly compute transmittance as well as the LAI (if both above and below light intensity readings are available). As Android device, we use the Samsung Galaxy Nexus with Android 4.2.2.

V. Field Trials

A. Study Area & Measurement Details

The maize field which was investigated from July to October during the growing season 2013 is located near the University of Osnabrück in the federal state of Lower Saxony in the north-western part of Germany. This field has a size of 3.5 ha. The mean annual precipitation of the study area is about 700 mm and the mean annual temperature is between 8 and 9 °C.

Four maize measurement campaigns were carried out on July 25^{th}, July 31^{st}, September 13^{th}, and October 08^{th}. During every campaign the LAI of 30–35 plots with different growth characteristics were measured to cover a wide range of LAI values. All measurements were only conducted between 10 am and 2 pm on days with a stable cloud cover to guarantee diffuse lightning conditions, which is a prerequisite for LAI assessment with the LAI-2200 device. Additionally, a 270 ° view cap (cf. [15]) was used to avoid any influence of the operator on the sensor of the LAI-2200 during the measurements. In every campaign, the TelosB device was installed directly on the measurement wand of the LAI-2200, close to the fish-eye optical sensor (Fig. 2(b)). One above and five below canopy readings were acquired at each plot to assess the transmittance and the LAI with the LAI-2200. From these readings, averaged transmittance and LAI values were directly calculated according to Equation 3 and 4. Simultaneous to the LAI-2200's above and below canopy readings, the TelosB samples incoming radiation at a rate of 3 Hz and transmits this data to the sink as described in Section IV-D.

B. Measurement Results

The goal of the measurement campaigns is to investigate the sensing accuracy of the COTS sensors for the LAI estimation using the results obtained by the LAI-2200 as reference and, thus, to validate the potential of these sensors for a large-scale and long-term agriculture deployment. We expected to achieve sufficient accuracy and the linear relation between the LAI estimates of both devices, similar to [20]. Since the LAI is derived from the transmittance, we initially considered the relation between the transmittance itself and expected it to be linear as well.

However, we could not assert this linear relationship as illustrated by the scatter plot in Figure 5(a). The scatter plot shows the transmittance values measured from the TelosB PAR sensor in all four campaigns and the corresponding LAI-2200 transmittance measurements. Moreover, there seems to be an exponential relationship between the measurements of both devices instead, which is underlined by a high coefficient of determination ($r^2 = 0.87$). The nonlinear relation between the transmittance measurements can be explained by the different spectral response ranges: TelosB: 320–730 nm (Sec. IV-A); LAI-2200: ≤ 490 nm (cf. Assumption 1 in Sec. IV-B). Furthermore, both sensors have different fields of view: TelosB: ≈ 180 °; LAI-2200: 148 °.

In a second step, we considered the LAI of both devices derived from the transmittance using Equation 2 and 4, respectively. In addition to the different fields of view, the LAI-2200 gains the transmittance of each ring with individual weighting factors in its LAI calculation (cf. Eq. 4) while the TelosB light sensor only provides a single measurement for the entire field of view. Note that although Gausman and Allen [9] have determined specific extinction coefficients (required in Eq. 2) at certain wavelengths for maize and other cultivars, the coefficient for the spectral range of the TelosB's PAR sensor was unknown and therefore could not be used for LAI calculation. Thus, we neglected the specific extinction coefficient by choosing $C = 1$.

When we considered the results of the first maize campaign (Fig. 5(b)), we surprisingly observed a strong linear relation ($r^2 = 0.92$) between TelosB and LAI-2200 measurements. However, the limited variations of plant development during first campaign causes a limited LAI range (0–3 measured by the LAI-2200) and is the reason of the linear relation presumed.

Figure 5(c) illustrates the combined measurement results of all maize campaigns. It is clearly shown that a wide LAI range induced by the inclusion of measurements of different phenological stages led to a nonlinear relationship between the LAI measurements which was already indicated by comparing the transmittances. The distribution of calculated LAI values from both devices indicated a logarithmic relation ($r^2 = 0.85$) between the measurements which again might be caused by the

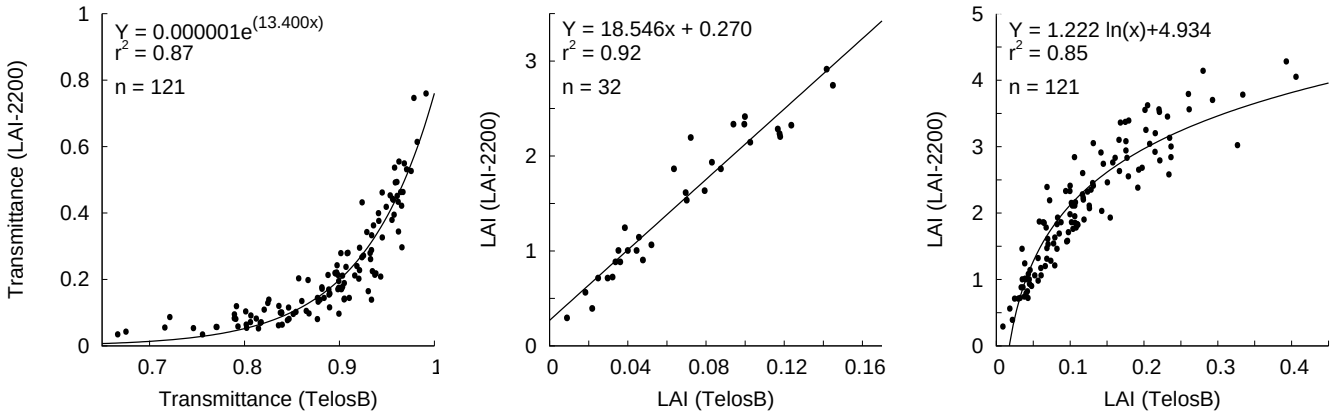

(a) Transmittance. (b) LAI (first maize campaign). (c) LAI (all maize campaigns).

Fig. 5. Correlation between estimates of TelosBs and the LAI-2200 instrument in the maize campaigns.

different visibility fields of both sensor devices. This nonlinear relation which is obviously independent from the chosen C was not expected due to the linear relation showed in [20] and led us to further investigations concerning the fields of view.

VI. Enhancement for the LAI Estimation

A. Adjusting the Field of View

Due to the nonlinear correlation observed between the results of the sensor node and the LAI-2200 instrument (Sec. V-B) and due to different fields of view of both platforms, we revised our measurement architecture. We decided to adjust the field of view of TelosB devices by mounting a little pipe directly onto the sensor (hereinafter referred to as *view pipe*). Figure 6 outlines the concept of this adjustment. The nearly 180 ° field of view of the TelosB's PAR sensor is restricted by two view pipes (7 ° and 23 ° limitation). Additionally, the five rings of the LAI-2200 instrument (cf. Fig. 1) are depicted to demonstrate that (1) the first ring of the LAI-2200 centered at 7 ° can be entirely emulated by the 7 ° view pipe (Fig. 6(a)) and (2) the subsequent rings can only be partially emulated. For instance, the 23 ° view pipe provides only a lower bound of the field of view at 28.6 ° but does not exclude the sector < 16.7 ° as done by the second ring of the LAI-2200 (Fig. 6(b)).

We believe that the simple approach of view pipes has the potential to enhance the WSN LAI estimation. As a proof of concept, we first conducted experiments in our lab followed by a second measurement campaign to investigate the impact of view pipes on the correlation with the LAI-2200.

In preliminary experiments, we determined the visibility field of the original and the modified PAR sensors using a laser pointer and varied the angle of incidence under lab conditions. Per incidence angle, we took roughly one hundred samples. The results of these experiments are shown in Figure 7(a) and confirm the intended effect, i.e., the field of view reduction matches approximately the lower bound of both rings. Moreover, Figure 7(b) depicts the setup used in the

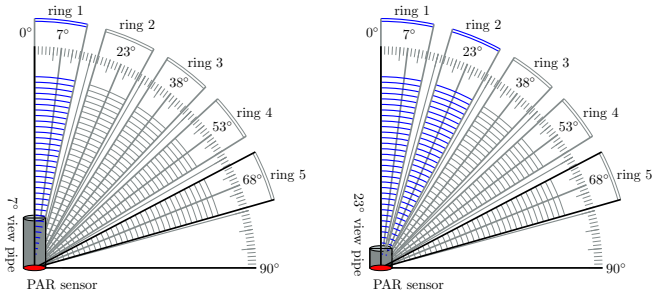

(a) The 7 ° view pipe corresponding to ring 1 of the LAI-2200. (b) The 23 ° view pipe corresponding to ring 1 and ring 2 of the LAI-2200.

Fig. 6. Concept of field of view adjustment using view pipes.

following campaign which consists of two TelosBs mounted on the LAI-2200 wand and modified by 7 ° and 23 ° view pipes. For time synchronization between both devices, we currently apply a loose synchronization which is achieved by mutually overhearing the 2 byte sequence numbers used in sensor data broadcasts, along with a possible adjustment.

B. Measurement Results

After the maize was harvested in November 2013, the measurements were alternatively continued on a year-round green leaf-bearing shrub. Two measurement campaigns were conducted on 17^{th} December 2013 and 31^{st} January 2014. The goal of the campaigns is to reinvestigate the relation between TelosB and LAI-2200 results concerning the transmittance as well as the LAI using the adjusted fields of view. By doing so, we intend to evaluate if (1) the nonlinear relation observed in Section V-B is caused by the different fields of view both devices have and (2) the view pipe approach has the potential to improve the LAI estimates from COTS sensor devices.

The measurement setup was similar to that used for the maize campaigns but the visibility field of the TelosB PAR sensor was adjusted with different view pipes. For the campaign in December 2013, the 7 ° view pipe was installed on TelosB sensor which reduces the field of view from approximately

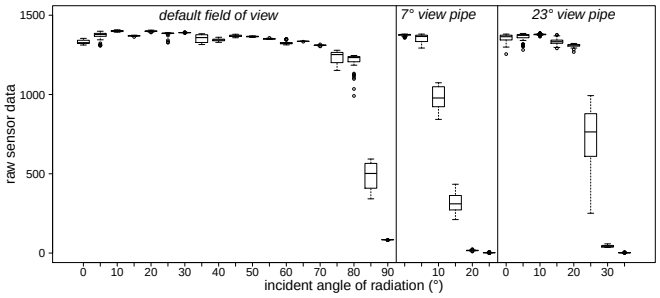

(a) Sensitivity depending on the incident angle of the original and modified sensors.

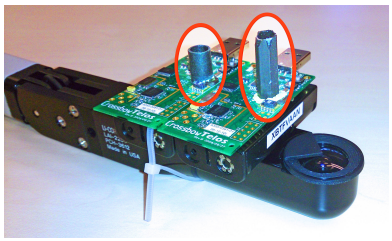

(b) Closeup view of modified TelosB nodes mounted on the LAI-2200 with view pipes (red ellipses).

Fig. 7. Practical realization of PAR sensors with adjusted fields of view using view pipes.

180 ° to 30 ° (= 2·15). This allows measurements comparable with those obtained by the first ring of the LAI-2200. Figure 8 illustrates the scatter plots of the transmittance and the LAI estimated by both devices. The transmittance (Fig. 8(a)) has a strong linear relation ($r^2 = 0.93$) and individual measurements lie close to the regression line. The observed gain (0.98) and offset (0.03) of the regression function indicate a comparable value range between the measurements of the TelosB and the LAI-2200. The LAI derived from the transmittance (Fig. 8(b)) covers a wide LAI range (0–7 measured by the LAI-2200) and also provide a robust linear model ($r^2 = 0.90$). Hence, the linear relation in both parameters clearly shows the benefit of the view pipe concept. Nevertheless, the LAI values obtained by the TelosB are much lower than the corresponding values of the LAI-2200, emphasized by the dashed line in Figure 8(b). This is caused by the chosen extinction coefficient $C = 1$ used in Equation 2. Figure 8(b) suggests a proper value of $C \approx 0.395$ for the specific cultivar with the spectral range of TelosB's PAR sensor in this measurement. However, the precise determination of this coefficient is very complex and out of our scope.

In January 2014, a second campaign was conducted using two TelosBs as shown in Figure 7(b). One TelosB sensor was again equipped with the 7 ° view pipe like it was done in the first shrub campaign. Again, this sensor was used to collect transmittance measurements comparable to those of the first LAI-2200 ring. On the second sensor, the 23 ° view pipe was installed emulating a visibility field of roughly 50 ° (= 2 · 25 , cf. Fig. 7(a)). The transmittance measurements of this sensor cover the field of view of the first and the second ring of the LAI-2200 optical sensor as discussed in Section VI-A.

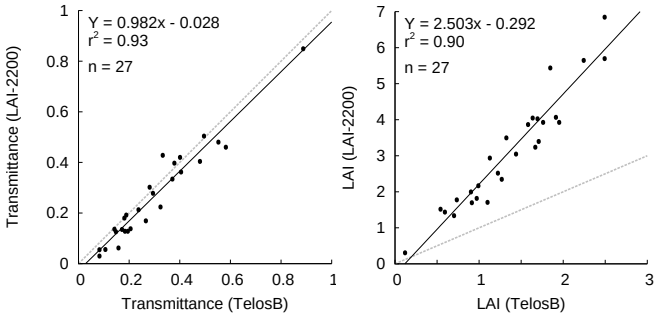

(a) Transmittance. (b) LAI.

Fig. 8. Correlation between estimates of a (modified) TelosB using the 7 ° view pipe versus LAI-2200 in the first shrub campaign.

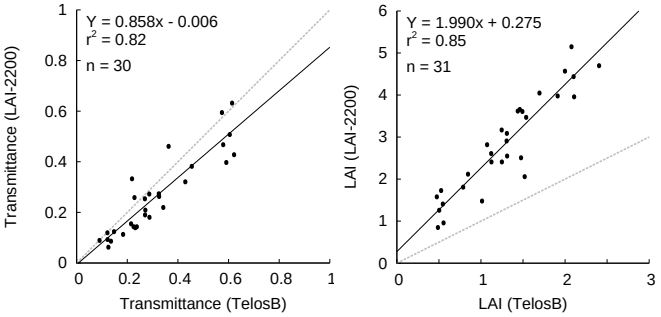

(a) Transmittance. (b) LAI.

Fig. 9. Correlation between estimates of a (modified) TelosBs using the 23 ° view pipes versus LAI-2200 in the second shrub campaign.

Therefore, we compare the results from the second TelosB sensor (23 ° view pipe) with the LAI-2200 results of both rings and use the corresponding weighting factors: 0.238 for the first and 0.762 for the second ring. The outcome of this comparison is shown in Figure 9.

Figure 9(a) illustrates the scatter plot for the transmittance measurements of the TelosB (23 ° view pipe) and the corresponding LAI-2200 measurements. Again, a clear linear relation between the measurements can be observed. However, the coefficient of determination ($r^2 = 0.82$) is lower compared to the coefficient which is obtained using the 7 ° view pipe, e.g., in the first shrub campaign. The reason for this lower accuracy achieved by the 23 ° view pipe is the fact that it does not exclude the sector $< 16.7°$ (cf. Sec. VI-A). Instead it combines both LAI-2200 rings by its entire 50 ° field of view. Thus, it is not possible to distinguish the light intensity in the sector $< 16.7°$ from the intensity in the sector $> 16.7°$ and to add the corresponding weightings. Consequently, this lower accuracy has a negative impact on the LAI and poses an inherent limitation of the view pipe approach which only provides lower bounds of the visibility field. However, the LAI has still the desired linear correlation ($r^2 = 0.85$) as shown in Figure 9(b).

VII. Conclusion and Future Work

In this paper, we investigated the potential of a common WSN platform (TelosB) for the in-field assessment of the leaf area index (LAI) which is one of the most important metrics to evaluate bio-physical crop characteristics. We described our experiences of indirect LAI estimation in various in-field measurement campaigns and directly compared the results achieved by the TelosB platform with those of a widely used standard instrument (LAI-2200). However, in contrast to related approaches, we were not able to observe a linear relation between both devices. Instead, we have shown that the nonlinear relation is induced by the nonrestrictive visibility field of TelosB's optical sensor. Furthermore, we proposed a view pipe approach and demonstrated its potential of rectifying this relation enabling a clear linear relation and comparable results if a proper extinction coefficient is assumed. Our evaluation shows very promising results concerning the first view pipe (7 °). However, we observed a lower accuracy for the second view pipe (23 °) which would be propagated by successive ones (38 °, 53 °, 68 °). Moreover, the evaluation reveals that the view pipe approach cannot entirely emulate the visibility field characteristics of the LAI-2200. Hence, the open research question is: Is it possible to achieve a sufficient accuracy as well as a linear correlation with a minimal set of sensors with specific view pipes?

In our future work, we will focus on this interesting question and intend to discover how many sensors and view pipes are required for a certain accuracy. We believe that the quantity and also the quality of view pipes will strongly depend on the specific crop type. Thus, we will investigate the view pipe approach in different crops during the growing season 2014. For that purpose, we plan to deploy a long-term agriculture WSN enabling data acquisition with high temporal and spatial resolution and to occasionally conduct destructive LAI measurements to further validate our results.

Acknowledgments

This work was supported by the "Stifterverband für die Deutsche Wissenschaft" (H170 5701 5020 20951).

References

[1] G. P. Asner, J. M. O. Scurlock, and J. A. Hicke, "Global synthesis of leaf area index observations: implications for ecological and remote sensing studies," *Global Ecology and Biogeography*, vol. 12, no. 3, pp. 191–205, 2003.

[2] E. Boegh, H. Soegaard, N. Broge, C. Hasager, N. O. Jensen, K. Schelde, and A. Thomsen, "Airborne multispectral data for quantifying leaf area index, nitrogen concentration, and photosynthetic efficiency in agriculture," *Remote Sensing of Environment*, vol. 81, no. 2–3, pp. 179–193, 2002.

[3] N. Bréda, "Ground-based measurements of leaf area index: a review of methods, instruments and current controversies," *Journal of Experimental Botany*, vol. 54, pp. 2403–2417, 2003.

[4] G. A. Carter, "Ratios of leaf reflectances in narrow wavebands as indicators of plant stress," *International Journal of Remote Sensing*, vol. 15, no. 3, pp. 697–703, 1994.

[5] J. M. Chen and T. A. Black, "Defining leaf area index for non-flat leaves," *Plant, Cell & Environment*, vol. 15, no. 4, pp. 421–429, 1992.

[6] C. Daughtry, K. P. Gallo, S. N. Goward, S. D. Prince, and W. P. Kustas, "Spectral estimates of absorbed radiation and phytomass production in corn and soybean canopies," *Remote Sensing of Environment*, vol. 39, no. 2, pp. 141–152, 1992.

[7] B. Duchemin, R. Hadria, S. Erraki, G. Boulet, P. Maisongrande, A. Chehbouni, R. Escadafal, J. Ezzahar, J. Hoedjes, M. Kharrou, S. Khabba, B. Mougenot, A. Olioso, J.-C. Rodriguez, and V. Simonneaux, "Monitoring wheat phenology and irrigation in Central Morocco: On the use of relationships between evapotranspiration, crops coefficients, leaf area index and remotely-sensed vegetation indices," *Agricultural Water Management*, vol. 79, no. 1, pp. 1–27, 2006.

[8] S. Garrigues, N. Shabanov, K. Swanson, J. Morisette, F. Baret, and R. Myneni, "Intercomparison and sensitivity analysis of Leaf Area Index retrievals from LAI-2000, AccuPAR, and digital hemispherical photography over croplands," *Agricultural and Forest Meteorology*, vol. 148, no. 8–9, pp. 1193–1209, 2008.

[9] H. W. Gausman and W. A. Allen, "Optical parameters of leaves of 30 plant species," *Plant Physiology*, vol. 52, no. 1, pp. 57–62, 1973.

[10] Hamamatsu, "Si photodiodes S1087/S1133 series," http://www.hamamatsu.com/resources/pdf/ssd/s1087_etc_kspd1039e02.pdf, Last checked: January 1, 2026.

[11] T. Jarmer, "Spectroscopy and hyperspectral imagery for monitoring summer barley," *International Journal of Remote Sensing*, vol. 34, no. 17, pp. 6067–6078, 2013.

[12] I. Jonckheere, S. Fleck, K. Nackaerts, B. Muys, P. Coppin, M. Weiss, and F. Baret, "Review of methods for in situ leaf area index determination: Part I. Theories, sensors and hemispherical photography," *Agricultural and Forest Meteorology*, vol. 121, no. 1–2, pp. 19–35, 2004.

[13] H. Kobayashi, Y. Ryu, D. D. Baldocchi, J. M. Welles, and J. M. Norman, "On the correct estimation of gap fraction: How to remove scattered radiation in gap fraction measurements?" *Agricultural and Forest Meteorology*, vol. 174–175, no. 0, pp. 170–183, 2013.

[14] K. Langendoen, A. Baggio, and O. Visser, "Murphy loves potatoes: experiences from a pilot sensor network deployment in precision agriculture," in *Proc. of 20th International Parallel and Distributed Processing Symposium (IPDPS '06)*, Rhodes Island, Greece, 2006.

[15] LI-COR, "LAI-2200 Plant Canopy Analyzer - Instruction Manual," http://www.licor.co.za/manuals/LAI-2200_Manual.pdf, Last checked: January 1, 2026.

[16] L. Mo, Y. He, Y. Liu, J. Zhao, S.-J. Tang, X.-Y. Li, and G. Dai, "Canopy closure estimates with GreenOrbs: sustainable sensing in the forest," in *Proc. of the 7th ACM Conference on Embedded Networked Sensor Systems (SenSys '09)*, Berkeley, CA, USA, 2009, pp. 99–112.

[17] M. Monsi and T. Saeki, "On the Factor Light in Plant Communities and its Importance for Matter Production," *Annals of Botany*, vol. 95, no. 3, pp. 549–567, 2005 (originally published in German, *Japanese Journal of Botany*, 1953).

[18] J. Polastre, R. Szewczyk, and D. Culler, "Telos: enabling ultra-low power wireless research," in *Proc. of the 4th International Symposium on Information Processing in Sensor Networks (IPSN '05)*, Los Angeles, CA, USA, 2005, pp. 364–369.

[19] Y. Qu and G. Sun, "Research on wireless sensor node for measurement of vegetation structure parameters," in *Proc. of the World Automation Congress (WAC '10)*, Kobe, Japan, 2010, pp. 437–442.

[20] Y. Qu, Y. Zhu, W. Han, J. Wang, and M. Ma, "Crop Leaf Area Index Observations With a Wireless Sensor Network and Its Potential for Validating Remote Sensing Products," *IEEE Journal of Selected Topics in Applied Earth Observations and Remote Sensing*, vol. 7, no. 2, pp. 431–444, Feb 2014.

[21] T. Shimojo, Y. Tashiro, T. Morito, M. Suzuki, D. Lee, I. Kondo, N. Fukuda, and H. Morikawa, "A Leaf Area Index visualization method using wireless sensor networks," in *Proc. of International Conference on Instrumentation, Control, Information Technology and System Integration Conference (SICE '13)*, Nagoya, Japan, 2013, pp. 2082–2087.

[22] M. van Ittersum, P. Leffelaar, H. van Keulen, M. Kropff, L. Bastiaans, and J. Goudriaan, "On approaches and applications of the Wageningen crop models," *European Journal of Agronomy*, vol. 18, no. 3–4, pp. 201–234, 2003.

[23] Y. Yuan, S. Li, K. Wu, W. Jia, and Y. Peng, "FOCUS: A cost-effective approach for large-scale crop monitoring with sensor networks," in *Proc. of the 6th International Conference on Mobile Adhoc and Sensor Systems (MASS '09)*, Macao, China, 2009, pp. 544–553.